RSC Advances

ROYAL SOCIETY OF CHEMISTRY

www.rsc.org/advances

RSC Advances

COMMUNICATION

An extreme high-performance ultraviolet photovoltaic detector based on ZnO nanorods/phenanthrene heterojunction†

Received 00th January 20xx,
Accepted 00th January 20xx

DOI: 10.1039/x0xx00000x

www.rsc.org/

Wentao Cheng,[a] Libin Tang,*[a,b] Jinzhong Xiang,*[a] Rongbin Ji,*[b] and Jun Zhao [b]

Ultraviolet (UV) photodetector is an important optoelectronic devices, the development of high-performance UV detector, however, has been impeded by lacking stable *p*-type wide-gap semiconductors. Here, an extremely high UV response for ZnO nanorods/phenanthrene(Phen) photovoltaic detector has been realized utilizing phenanthrene as a *p*-type wide-gap organic semiconductor, a detectivity (*D) as high as ~9.0×10^{13} cm Hz$^{1/2}$ W^{-1} has been reached, showing significant potential optoelectronic applications.**

Introduction

Ultraviolet (UV) photodetector is a kind of important optoelectronic device which can be widely used in fire warning,[1–3] environmental monitoring,[4–6] missile approach warning,[7, 8] ultraviolet communication,[9–11] astronomical observation,[12] missile guidance,[13] *etc*. Photovoltaic detector has a number of advantages including larger array, lower power consumption, faster response, simpler integration with ROIC *etc*. over the photoconductive device. However, the development of UV photovoltaic device has been impeded by lacking *p*-type wide-gap semiconductors, making it difficult to fabricate photovoltaic detectors.

In this communication, a novel UV photovoltaic (PV) detector has been designed and fabricated using ZnO nanorods and phenanthrene as *n*-type and *p*-type UV sensitive materials, respectively. ZnO nanorods that vertically grown on the bottom electrode ITO play two important roles in the device, one is to absorb UV light, the other is to transport photogenerated carriers higher efficiently. The other important material phenanthrene in this device functionalized as UV light absorber and photogenerated-hole transporter. Importantly, a detectivity (*D**) as high as ~9.0×10^{13} Jones (1 Jones =1 cm Hz$^{1/2}$ W^{-1}) has been reached for our un-optimized device,[14] the performance of our UV PV detector is superior to the conventional UV detectors, showing significant potential applications in UV optoelectronics devices.

[a] School of Physical Science and Technology, Yunnan University, Kunming, 650091, P. R. China. Email: scitang@163.com, jzhxiang@ynu.edu.cn.
[b] Kunming Institute of Physics, Kunming, 650223, P. R. China. Email: scitang@163.com, jirongbin@gmail.com

† Electronic Supplementary Information (ESI) available: The performance comparison of the ZnO Nanorods/Phen UV detector with some common UV detectors. See DOI: 10.1039/x0xx00000x

Experimental section

All the chemical reagents used in the experiments were used as received without further purification. Zinc acetate dihydrate (99%) was purchased from Tianjin BoDi Chemical Co., Ltd., phenanthrene was purchased from Tianjin Guangfu Fine Chemical Research Institute, hexamethylenamine (99%) was purchased from Tianjin FengChuan Chemical Reagent Technologies Co., Ltd. The details of solvents and other chemicals are listed in ESI.

Indium tin oxide (ITO) glass substrates (30 Ω/*sq*) were rinsed in an ultrasonic bath with detergent, acetone, ethanol for 15 min, sequentially, followed by rinsing with deionized water (DI) several times. ZnO seed layer was prepared on ITO substrate by spin-coating of sol-gel solution (2 g zinc acetate dehydrate dissolved in a mixture solvent of 60 mL ethanol, 1 mL ethanolamine, 2 mL ethylene glycol and 1 mL glacial acetic acid), then annealed at 400℃ for 2 h in the air. ZnO nanorods were grown on ZnO seed layer in the 0.02 mol L^{-1} zinc acetate dihydrate: hexamethylenetetramine (mole ratio 1:1) solution at 90□ for 6 h, then rinsed with DI water several times. The ZnO Nanorods/Phen heterojunciton was fabricated by spin-coating ZnO nanorods with 0.2 mL phenanthrene solution (2.5g L^{-1}, solvent: ethanol), then the heterojunction was placed in an oven heated at 50□ for 20 min. Finally, the heterojunction was coated with silver paste (1mm^2) as the top electrode.

The morphology and the nano-texture of the active layer and the detector were examined by scanning electron microscope (SEM, Hitachi S-3400N). The X-ray diffraction (XRD) patterns of the samples were measured by Rigaku D/Max-23 at room temperature. The transmission electron microscope (TEM) and high-resolution TEM (HRTEM) characterizations were performed using the JEOL JEM-2100 transmission electron microscope. The current density-voltage (*J-V*) characteristics were tested with a Keithley 2400 source meter. The Raman scattering spectrum was recorded at ambient

temperature using a Renishaw inVia Raman microscope with an argon-ion laser at an excitation wavelength of 514.5 nm. The UV-Vis absorption spectra were recorded by a Shimadzu UV-2401 PC spectrometer. The photoluminescence (PL) emission and Photoluminescence excitation spectra were recorded using a Hitachi F-4500 spectrometer.

Results and discussion

We have designed a novel structure to upgrade the performance of UV detector, Fig. 1 is the energy band diagram of the device, in which we choose ZnO Nanorods/Phen heterostructure as the composite photoactive material, where phenanthrene is acted as an UV absorbing, photogenerated-hole transporting and collecting layer.[15, 16]

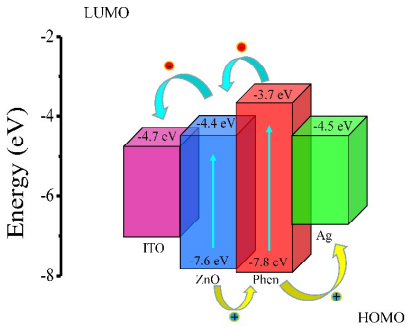

Fig. 1 The schematic diagram of energy band for the ZnO/Phen UV organic photovoltaic detector.

The ZnO/Phen UV organic photovoltaic (OPV) detectors were fabricated as shown in Fig. 2, firstly, ITO/glasses were ultrasonically rinsed by acetone, ethanol, DI water sequentially. The ZnO seed layer was prepared at 400℃ for 2h by a sol-gel method, the ZnO nanorods were grown vertically on the ZnO seed layer at 90℃ for 6h. Then phenanthrene was deposited on ZnO nanorods by spin-coating phenanthrene solution onto ZnO nanorods. Finally, the metal electrodes were deposited onto the ZnO Nanorods/Phen heterostructure. The vertical structure of device facilitates photocarriers collection.

The structure of the ZnO Nanorods/Phen UV OPV detector is schematically shown in Fig. 3a, ITO and Ag were acted as bottom and top electrodes, respectively. The SEM image of the ZnO Nanorods/Phen heterostructure was shown in Fig. 3b, the deposition of Phen on ZnO nanorods does not change the morphology of ZnO nanorods observably. The SEM cross-section image of the ZnO Nanorods/Phen heterostructure was shown in Fig. 3c, it is obvious that the heterostructure is perpendicular to the ITO, the length of ZnO nanorods is ~ 2.8μm, the thickness of ITO is 180 nm.

The XRD pattern of the ZnO Nanorods/Phen heterostructure is shown in Fig. 3d, the strongest diffraction peak is ZnO (002) located at (2θ =34.46 °), showing that ZnO nanorods were grown

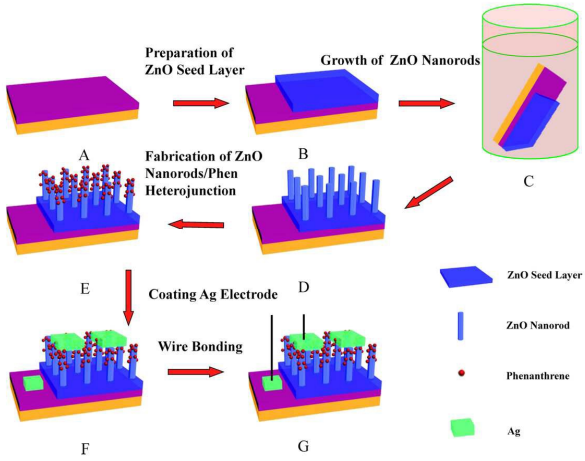

Fig. 2 The schematic illustration of the fabrication process for the ZnO/Phen UV OPV detector. The devices were fabricated on ITO substrates, briefly, ZnO seed layer was prepared on ITO by sol-gel method, ZnO nanorods were grown on the seed layer by chemical solution method at 90℃ for 6 h, the ZnO Nanorods /Phen heterostructure was prepared by spin-coating phenanthrene solution onto ZnO nanorods, the metal electrode was deposited onto the heterostructure.

perpendicularly to the substrate. The phenanthrene (001) diffraction (2θ =9.32 °) has also been observed.

As shown in Fig. 3e, the *J-V* curves of ZnO Nanorods/Phen UV OPV detector show good rectifying properties both in the dark and under UV illumination.

Importantly, it is found that the ZnO Nanorods/Phen UV OPV detector shows a remarkable increase in current density under an UV illumination (λ=365 nm) with a power density of 1.650 mW cm^{-2} (Fig. 3e), which means that the detector may exhibit an excellent device performance.

A series of UV light power densities (0, 0.002, 0.175, 0.550, 1.350 and 1.650 mW cm^{-2}) have been used to illuminate the detector to test the device performance, as shown in Fig. 3f that the current density increases with UV light power density.

Fig. 4a is the SEM image of the ZnO nanorods on the substrate, it is obvious that the nanorods were grown vertically on the substrate, the end of rods takes on a hexagon shape. Fig. 4b is the XRD pattern of ZnO nanorods array, it can be observed that both (103) and (004) diffraction peaks are rather weak compared to (002) diffraction peak, indicating the nanorods were preferably grown along (002) orientation.

The Raman spectrum of ZnO nanorods is shown in Fig. 4c, obviously, there are two vibration peaks centered at 439 and 1095 cm^{-1}, respectively, corresponding to (E_{2H}, TO) and (E_{1L}, 2LO) vibration modes.[17–19] Fig. 4d and 4e are the TEM images of ZnO nanorods under different magnifications, it can be seen that the diameters of the nanorods are uniform, the typical diameter is ~ 70-80nm. The lattice fringes of ZnO can be clearly observed in Fig. 4f, showing good crystalline structure of ZnO nanorods, the spacing between the fringes is 0.261nm, which is the crystal plane spacing of *c* axis, meaning that the growth direction of the nanorods are along (002) orientation. The fast Fourier transform

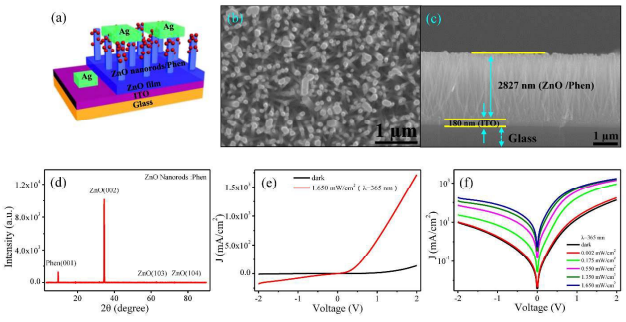

Fig. 3 (a) The schematic diagram of the ZnO/Phen UV OPV detector. (b) The SEM image of the ZnO nanorods/phenanthrene heterostructure. (c) The SEM corss-section image of the ZnO nanorods/phenanthrene heterostructure. (d) The XRD pattern of the ZnO nanorods/phenanthrene heterostructure. (e) The *J-V* curves of the ZnO/Phen UV OPV detector in the dark and under the illumination of 365 nm UV LED with a power density of 1.650 mW cm^{-2}, respectively. (f) The effect of UV power density (λ=365 nm) on the ZnO/Phen UV OPV detector.

of the selected area (red square) is shown in the inset of Fig. 4f, the hexagonal wurtzite structure has been demonstrated.[20] Fig. 4g is the electron diffraction (ED) pattern of the ZnO nanorods, many diffraction spots have been observed, corresponding to (002), (004) and (103) diffraction planes, respectively. It can also be seen that the strongest plane is (002).

Fig. 5a is the UV-Vis absorption spectra for phenanthrene solution samples, it can be observed that phenanthrene has a strong UV absorption ranged in 200-300 nm, both ethanol and methanol phenanthrene solutions show similar spectra. The UV-Vis absorption spectra for ZnO nanorods and ZnO Nanorods/Phen are shown in Fig. 5b, clearly, there is an absorption peak located at ~375 nm for both ZnO nanorods and

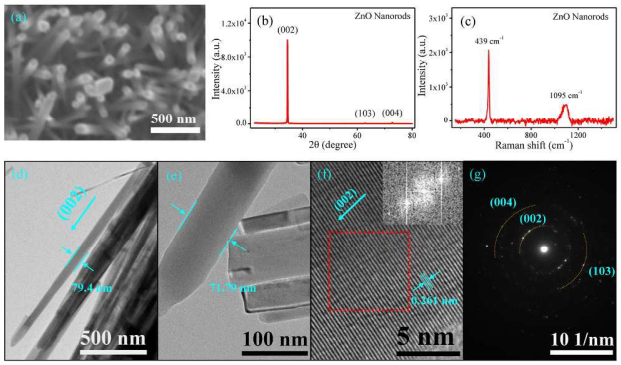

Fig. 4 (a) The SEM image of the ZnO nanorods array. (b) The XRD pattern of the ZnO nanorods array. (c) The Raman spectrum of the ZnO nanorods array measured at room temperature (λ_{exc}=514.5 nm). (d) and (e) The TEM images of ZnO nanorods under different magnifications. (f) The HRTEM image of a single ZnO nanorod. Inset: the FFT pattern of the selected area (red square). (g) The electron diffraction (ED) pattern of the ZnO nanorods.

the hybrid heterostructure. This peak is resulted from the exciton absorption.

The photoluminescence (PL) spectra of ZnO nanorods were measured using a series of excitation wavelength (λ_{ex}) (250, 280, 300, 330, 360 nm). The PL emission peaked at ~ 400 nm, the wavelength is longer than UV absorption, due to stokes shift (Fig. 5c). The visible PL emission is correlated with defects of ZnO nanorods.[21, 22] The PL excitation (PLE) spectra were measured at a number of receiving energies (λ_{em}) (400, 420, 450, 480, 530 nm) as shown in Fig. 5d, the PLE peak locates at ~237 nm.

The phenanthrene doped ZnO nanorods show enhanced PL emission compared with undoped ZnO nanorods, as shown in Fig. 5e, the PL emission spectrum presents a λ_{ex} dependent properties, a shorter (240 nm) or longer (360 nm) λ_{ex} cannot result in the strongest PL emission, only at a proper λ_{ex} (*e.g.* 270 nm) may lead to the strongest emission. Fig. 5e also shows similar shape (multipeak) in PL emission spectra under different λ_{ex}, the multi-peaks of the heterojunction are mainly resulted from the multi electron transitions from the ZnO/Phen heterojunction where Phen contains a number of the molecular orbital energy levels. Phenanthrene-sensitised ZnO nanorods also show dissimilar PLE spectra, the PLE peaks of the heterojunction are red-shifed to ~290nm compared to ZnO nanorods (~237 nm) as shown in Fig. 5f.

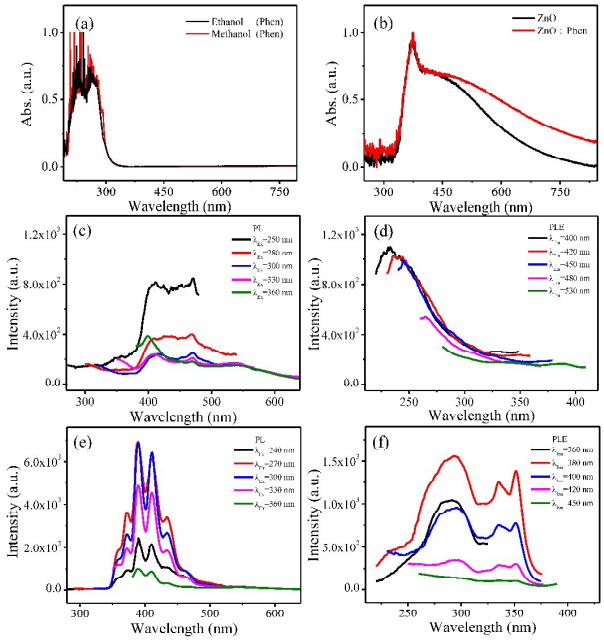

Fig. 5 (a) The UV-Vis absorption spectra of phenanthrene in ethanol and methanol. (b) The UV-Vis absorption spectra of ZnO nanorods and ZnO nanorods/phenanthrene heterostructure. (c) The PL emission spectra of ZnO nanorods. (d) The PL excitation spectra of ZnO nanorods. (e) The PL emission spectra of ZnO Nanorods/Phen heterostructure. (f) The PL excitation spectra of ZnO Nanorods/Phen heterostructure.

The novel heterojunction based UV detector shows a very good performance, a series of power densities of UV LED light (365 nm) were used to illuminate the device, as shown in Fig. 6a, under a forward bias voltage, the responsivity (R) ($R = J_{ph}/L_{light}$)[14, 23] increases with reducing in UV light power density, the highest responsivity reaches ~ 2.0×10^4 A W^{-1} (0.002 mW cm^{-2}), which is the highest reported value compared to the common UV detectors. [24, 25] The effect of Phen thickness on the device performance has also been investigated, it is found that a thinner or a thicker Phen film is not effective for the photon-absorption (thinner film), the transport and collection of photon-generated carriers (thicker film). Only a proper thickness of Phen in the heterojunction may get the high performance（as shown in Fig. S1 of the ESI）.

Fig. 6b shows the effect of bias voltage on the responsivity of device, it can be clearly seen that a bigger bias voltage results in a larger responsivity, probably due to the photo-generated carriers may be more efficiently collected at a higher bias voltage.

Detectivity (D^*) is an important parameter to evaluate the performance of photodetector. D^* is defined as follows, $D^*= R/(2qJ_d)^{1/2} =(J_{ph}/L_{light})/(2qJ_d)^{1/2}$. Fig. 6c shows that D^* increases with increasing of bias voltage, the highest D^* reaches ~9.0×10^{13} Jones which is the highest performance compared with ZnO based UV detectors (see ESI). It is also found that the illumination power density may affect D^*, for our device D^* increases with decreasing the illumination power density, meaning that our device is suitable for detecting week UV signal.

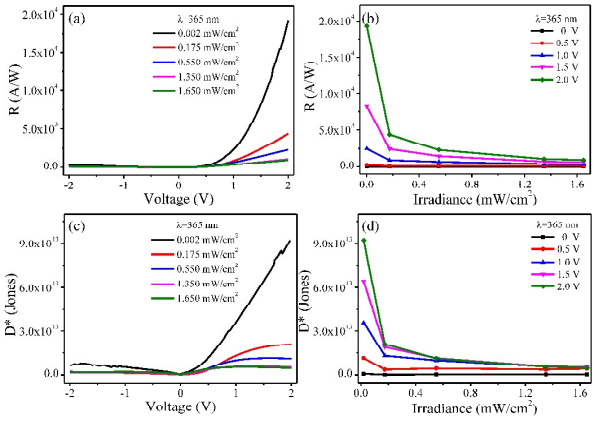

Fig. 6 The room-temperature device performances of the ZnO/Phen UV OPV detector. (a) The effect of UV illumination power density (λ=365 nm) on responsivity (R). (b) The effect of bias voltage on responsivity (R). (c) The effect of UV illumination power density (λ=365nm) on detectivity (D^*). (d) The effect of bias voltage on detectivity (D^*).

Conclusions

In summary, a novel UV photovoltaic detector based on ZnO nanorods/phenanthrene heterojunction has been designed and fabricated, where ITO and Ag have been used as the bottom and top electrodes. ZnO nanorods grown vertically on ITO were served as UV light absorber and photogenerated carriers transport layer. Phenanthrene is functioned as both UV sensitive layer and hole transport layer. The device is very sensitive to UV light, reaching a detectivity (D^*) as high as ~9.0×10^{13} cm $Hz^{1/2}$ W^{-1}, which is extremely high compared with conventional UV detectors. This study paves the way for fabricating high-performance, low-power-consumption, large-array, fast-response UV focal plane array detector.

Acknowledgements

This work was supported by National Natural Science Foundation of China (No. 61106098, 51201150), and the Key Project of Applied Basic Research of Yunnan Province, China (No. 2012FA003).

Notes and references

1 D. Walker, X. Zhang, P. Kung, A. Saxler, S. Javadpour, J. Xu and M. Razeghi, *Appl. Phys. Lett.*, 1996, **68**, 2100–2101.
2 T. Tut, M. Gokkavas, A. Inal and E. Ozbay, *Appl. Phys. Lett.*, 2007, **90**, 163506.
3 M. Razeghi and A. Rogalski, *J. Appl. Phys.*, 1996, **79**, 7433–7473.
4 S. J. Young, L. W. Ji, S. J. Chang and Y. K. Su, *J. Cryst. Growth*, 2006, **293**, 43–47.
5 A. G. Ardakani, M. Pazoki, S. M. Mahdavi, A. R. Bahrampour and N. Taghavinia, *Appl. Surf. Sci.*, 2012, **258**, 5405–5411.
6 X. D. Li , C. T. Gao , H. G. Duan , B. G. Lu , Y. Q. Wang , L. L. Chen , Z. X. Zhang , X. J. Pan and E. Q. Xie, *Small*, 2013, **9**, 2005–2011.
7 P. Sandvik, K. Mi, F. Shahedipour, R. McClintock, A. Yasan, P. Kung and M. Razeghi, *J. Cryst. Growth*, 2001, **231**, 366–370.
8 J. S. Liu, C. X. Shan, B. H. Li, Z. Z. Zhang and C. L. Yang et al, *Appl. Phys. Lett.*, 2010, **97**, 251102.
9 C. H. Chen, S. J. Chang, S. P. Chang, M. J. Li, I. C. Chen, T. J. Hsueh and C. L. Hsu, *Chem. Phys. Lett.*, 2009, **476**, 69–72.
10 E. Monroy, F. Omnès and F Calle, *Semicond. Sci. Technol.*, 2003, **18**, R33–R51.
11 Y. A. Goldberg, *Semicond. Sci. Technol.*, 1999, **14**, R41-R60.
12 L. Peng, L. F. Hu and X. S. Fang, *Adv. Mater.*, 2013, **25**, 5321–5328.
13 S. M. Hatch, J. Briscoe and S. Dunn, *Adv. Mater.*, 2013, **25**, 867–871.
14 X. Gong, M. H. Tong, Y. J. Xia, W. Z. Cai, J. S. Moon, Y. Cao, G. Yu, C. L. Shieh, B. Nilsson and A. J. Heeger, *Science*, 2009, **325**, 1665–1667.
15 G. Malloci, G. Cappellini, G. Mulas and A. Mattoni, *Chem. Phys*., 2011, **2978**, 1–26.
16 T. Kato, K. Yoshizawa and K. Hirao, *J. Chem. Phys.*, 2002, **116**, 3420–3429.
17 T. C. Damen, S. P. S. Porto and B. Tell, *Phys. Rev.*, 1966, **142**, 570–574.
18 H. M. Cheng, H. C. Hsu, Y. K. Tseng, L. J. Lin and W. F. Hsieh, *J. Phys. Chem. B*, 2005, **109**, 8749–8754.

19 R. C. Lima, L. R. Macario, J. W. M. Espinosa, V. M. Longo, R. Erlo, N. L. Marana, J. R. Sambrano, M. L. dos Santos, A. P. Moura, P. S. Pizani, J. Andrés, E. Longo and J. A. Varela, *J. Phys. Chem. A*, 2008, **112**, 8970–8978.
20 G. Z. Shen, Y. Bando, B. D. Liu, D. Golberg and C. J. Lee, *Adv. Funct. Mater.*, 2006, **16**, 410–416.
21 X. D. Wang, C. J. Summers and Z. L. Wang, *Nano Lett.*, 2004, **4**, 423–426.
22 X. W. Sun, J. Z. Huang, J. X. Wang and Z. Xu, *Nano Lett.*, 2008, **8**, 1219–1223.
23 F. W. Guo, B. Yang, Y. B. Yuan, Z. G. Xiao, Q. F. Dong, Y. Bi and J. S. Huang. *Nat. Nanotechnol.*, 2012, **7**, 798–802.
24 Q. Yang, X. Guo, W. H. Wang, Y. Zhang, S. Xu, D. H. Lien and Z. L. Wang, *ACS Nano*, 2010, **4**, 6285–6291.
25 G. Konstantatos and E. H. Sargent, *Nat. Nanotechnol.*, 2010, **5**, 391–400.